



# Terahertz Quality Inspection for Automotive and Aviation Industries

F. Ellrich<sup>1</sup> · M. Bauer<sup>2</sup> · N. Schreiner<sup>2</sup> · A. Keil<sup>2</sup> · T. Pfeiffer<sup>2</sup> · J. Klier<sup>2</sup> · S. Weber<sup>2</sup> · J. Jonuscheit<sup>2</sup> · F. Friederich<sup>2,3</sup> · D. Molter<sup>2</sup>

Received: 19 June 2019 / Accepted: 21 October 2019 / Published online: 26 November 2019  
© The Author(s) 2019

## Abstract

Nondestructive quality inspection with terahertz waves has become an emerging technology, especially in the automotive and aviation industries. Depending on the specific application, different terahertz systems—either fully electronic or based on optical laser pulses—cover the terahertz frequency region from 0.1 THz up to nearly 10 THz and provide high-speed volume inspections on the one hand and high-resolution thickness determination on the other hand. In this paper, we present different industrial applications, which we have addressed with our terahertz systems within the last couple of years. First, we show three-dimensional imaging of glass fiber–reinforced composites and foam structures, and demonstrate thickness determination of multilayer plastic tube walls. Then, we present the characterization of known and unknown multilayer systems down to some microns and the possibility of measuring the thickness of wet paints. The challenges of system reliability in industrial environments, e.g., under the impact of vibrations, and effective solutions are discussed. This paper gives an overview of state-of-the-art terahertz technology for industrial quality inspection. The presented principles are not limited to the automotive and aviation industries but can also be adapted to many other industrial fields.

**Keywords** Terahertz · Quality inspection · Automotive · Aviation · Volume inspection · Composite material characterization · Foam inspection · Layer thickness determination · Multilayer · Wet coatings · Vibration compensation

✉ F. Ellrich  
f.ellrich@th-bingen.de

<sup>1</sup> Department 2 - Technics, Informatics and Industrial Engineering, TH Bingen, University of Applied Sciences, Berlinstr. 109, 55411 Bingen, Germany

<sup>2</sup> Center for Materials Characterization and Testing, Fraunhofer Institute for Industrial Mathematics ITWM, Fraunhofer-Platz 1, 67663 Kaiserslautern, Germany

<sup>3</sup> Department of Physics and Research Center OPTIMAS, University of Kaiserslautern, 67663 Kaiserslautern, Germany

## 1 Introduction

In the recent years, impressive developments from the terahertz community have shown that terahertz technology is a very attractive tool to complement well-established methods in the field of nondestructive testing [1–8]. The unique characteristics of terahertz radiation, e.g., being nonhazardous and providing high-contrast images when penetrating dielectrics (compared, e.g., with X-ray techniques) combined with a higher resolution than microwaves, have led to many different applications, especially in the automotive and aviation sectors. Following the study of TEMATYS SARL [9], the market size of nondestructive testing with terahertz radiation in 2012 was comparable with the size of terahertz research at these times. Until 2020, the study predicted a doubling of the industrial market compared with the research volume, while assuming that the overall terahertz market increases with 16% per annum. Most probably, there will not be an abrupt change from existing and reliably working solutions in industrial production lines even when the terahertz solution is able to serve additional values at the same time. Mostly implemented as an additional technology parallel to already-implemented quality inspections systems today, terahertz measurement techniques could gradually lead to fully terahertz-controlled processes. Here, challenges given by rough industrial environments in comparison with research laboratories must be overcome. The largest and most attractive industrial application at the moment is the thickness measurement technology [9, 10]. In cooperation with several industrial partners, we have already solved a number of practical problems, e.g., the vibration of objects during high-precision thickness measurements. Using interferometric-controlled real-time distance information, we were able to eliminate the impact of such vibrations almost completely. Hence, we realized a reliable terahertz-based thickness gauge being able to resolve multilayer systems of, e.g., car bodies in the production line.

Terahertz solutions have proven highly attractive in particular for material characterization of novel and complex materials, where state-of-the-art testing technologies often do not work or at least their employment is highly restricted. In the context of the energy revolution, especially, the automotive and aviation industries are in search for new materials, which provide sufficient structural stability and are lightweight in comparison with, e.g., metal-based constructions. Fiber-reinforced composite materials made of multiple layers of carbon, glass, natural fibers, etc. are on the rise. Here, terahertz technology is able to support the quality inspection of such structures in two ways. On the one hand, volumetric inspection of the materials to identify possible inclusions, cracks, or other defects is of high interest. This is done, e.g., for radomes typically constructed out of glass fiber-reinforced plastics (GFRP) forming a protecting shell for radar antennas. A high degree of transparency of radomes is essential to ensure proper signal transmission. We developed a terahertz inspection system for the radome production industries, which inspects this critical part of the radar transmission link for aircrafts. On the other hand, the thickness of the coatings protecting the composite structures has to be controlled. Well-established methods based on eddy-current or photothermic principles often fail for composite substrates, whereas the substrate-independent terahertz technology for thickness measurements meets these demands.

The terahertz technologies presented in this paper can be roughly divided into two categories. In the first part of this paper (section 2), we demonstrate electronic, fast-scanning, frequency-modulated continuous-wave (FMCW) technology, employed mainly for applications focusing on volume inspection of composites and foam structures. In addition, thickness information of layer systems in the millimeter range can be gathered with this technology. In

the second part of the paper (section 3), we present optical terahertz systems based on the time-domain spectroscopy (TDS) principle for precise measurement of thin layers down to several microns. The measurement principle itself, the challenges arising with the implementation of the technology under industrial conditions, and the generated solutions are described. The final section—section 4—gives a conclusion and an outlook of terahertz technologies used for quality inspection in the automotive and aviation industries.

## 2 Volume Inspection

Millimeter wave and terahertz imaging systems have proven to be highly attractive for contactless inspections beneath the surface of dielectric structures. In this context, they are complementary to other established imaging techniques for nondestructive testing, which was investigated in some detail in the EU-funded DOTNAC project [11]. Exhaustive comparative measurements on glass fiber–reinforced plastic (GFRP) composites with artificial defects showed that FMCW terahertz transceivers (for details on the measurement principle, see section 2.1) operated between 75 and 320 GHz can exhibit superior performance for the inspection of multilayer structures with foam and/or honeycomb cores [12, 13]. In particular, the terahertz measurements were compared with measurements by thermography and ultrasound techniques—pulse echo and inverse wave field extrapolation (IWEX)—in reflection geometry, as well as X-ray radiography and ultrasound transmission measurements. Figure 1a shows a schematic of one of the test sample geometries with the artificial defect locations indicated in red. The defects—represented by air gaps and polytetrafluoroethylene (PTFE) and paper inlays—were positioned at different depths of the sample on top of the honeycomb core structure: between the covering glass fiber laminate plies, between the laminate structure and the adhesive resin on the honeycomb core, as well as between the adhesive and core. The lateral location of the defects is visualized in Fig. 1b with the help of an exemplary terahertz image acquired at 150 GHz operation frequency. The evaluation of defect detection rates shown in Fig. 1c corroborates that only the FMCW terahertz system performs well in single-side-access reflection measurements both from the top and from

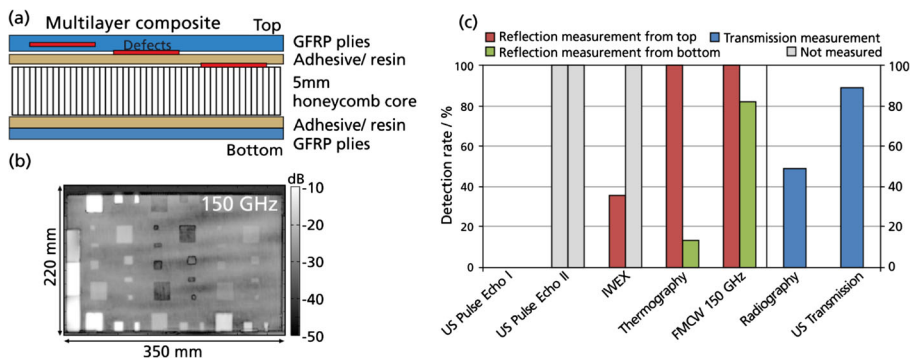


**Fig. 1** **a** Schematic of a composite structure containing layers of GFRP, adhesive, and a honeycomb core. **b** Reflection image at 150 GHz of implemented defects in a GFRP laminate sample. **c** Detection rate of various nondestructive testing technologies for implemented defects in GFRP composite test samples. Test results from the EU DOTNAC project [11]

the bottom through the honeycomb core. The defect detection rate could be further improved by semi-automated defect detection via data conditioning and image processing as described in [14].

## 2.1 FMCW Terahertz Measurements

The FMCW technique is a measurement approach enabling depth-resolved volume inspection with the help of a frequency-tunable continuous-wave radiation source. Figure 2a shows an illustration of the FMCW measurement principle. Linear frequency-modulated signals are generated within the source and transmitted (Tx) to illuminate a target under investigation. The waves are reflected (Rx) at the target's surface and—for terahertz-transparent materials—at each material interface within the target. The reflected signals are each shifted in time with respect to the generated frequency ramps serving as a local oscillator reference. Heterodyne mixing of the reference with the received reflection signals leads to a beat frequency signal  $f_b$ , which can be sampled directly by a data acquisition unit (DAQ) and which, via Fourier transform, relates the detected beat frequency to a time-of-flight  $\tau$  directly correlated with a range distance  $d$  of the reflecting interface [15]

$$d = \frac{c}{2n} \tau = \frac{c f_b T_{\text{sweep}}}{2nB}, \quad (1)$$

with  $n$  the refractive index of the material,  $c$  the speed of light in vacuum, and  $B$  the total sweep bandwidth. While the lateral resolution of terahertz imaging systems is limited by the employed wavelength in connection with the focusing optics, the Rayleigh criterion for the depth resolution  $\Delta r$  is determined by the bandwidth  $B$  of the frequency modulation of the FMCW system as

$$\Delta r = \frac{c}{2nB}. \quad (2)$$

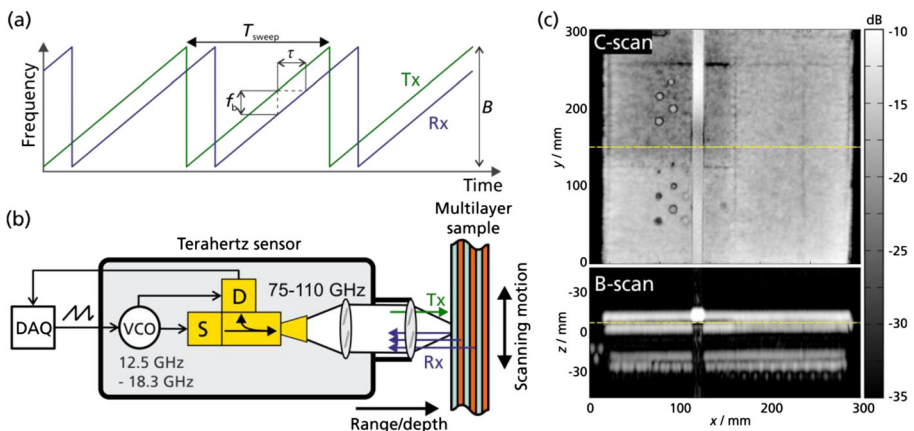


**Fig. 2** **a** Illustration of the FMCW measurement principle. **b** Typical setup of a FMCW terahertz transceiver. **c** Terahertz images (C-scan and B-scan) of a GFRP composite test panel with implemented sub-surface defects of various diameters

Figure 2b shows a schematic of the implementation of an all-electronic FMCW terahertz measurement unit (here, W-band system with a center frequency of 100 GHz). Linear frequency ramps are generated in the low-frequency K-band with a DAQ-controlled voltage-controlled oscillator (VCO) and converted into the terahertz range by an active frequency multiplier chain (S)—in the illustration example with a multiplication factor of 6. The frequency-modulated terahertz wave is then transmitted (Tx) by a conical horn antenna and the same antenna also receives the reflection signals (Rx) from the sample under test. An attached directional coupler feeds the received signals to a Schottky diode-based receiver (D) where they are mixed with the reference frequency ramps to obtain the beat signals. The latter are sampled by a DAQ for further processing in a computer for the reconstruction of depth information of the sample under test.

The measurement systems developed in our group typically operate at center frequencies of 90, 140, 270, and 410 GHz providing bandwidths of 40, 60, 100, and 180 GHz, respectively. For imaging purposes, our monostatic transceivers are commonly operated in connection with motion systems and with a quasi-optical lens or mirror setup in order to focus the terahertz radiation to a measurement spot and to guide the reflected signals back into the transceiver, as indicated in the scheme in Fig. 2b. The optical configuration defines the focal spot size as well as the depth of focus of the terahertz beam. Hence, depending on the intended application, a careful consideration of the optical setup is required.

As an example for a typical image obtained with a FMCW terahertz measurement system, Fig. 2c shows the C- and B-scans of an inner layer of a 2-cm-thick and  $50 \times 50 \text{ cm}^2$  large GFRP multilayer sample. The yellow line in the B-scan image indicates the ( $z$ )-location of the shown C-scan image and vice versa. The composition of different panels within the sample as well as internal defects can well be recognized within both the B- and C-scan images. While the motion of a single-point sensor limits the acquisition time for volumetric images significantly, multistatic array configurations in connection with digital beam forming techniques, as described in section 2.4, can provide faster operation and a proper solution to this limitation.

The example proves that the FMCW approach in connection with terahertz and millimeter waves allows a volumetric inspection and three-dimensional localization of defects and/or material layers within terahertz-transparent samples. The following sections address a number of specific application scenarios of FMCW terahertz measurements.

## 2.2 Radome Inspection

A number of successful applications of FMCW millimeter wave and terahertz systems for the inspection of radomes have been demonstrated. Besides requirements on their structural integrity, the radome's electromagnetic properties with regard to the embedded radar systems are of significant relevance for their design. In [16], e.g., the radiation characteristics of automotive radomes, which are typically strongly influenced by aesthetic aspects of the chassis design, were investigated using a stepped-frequency continuous-wave measurement system working around 77 GHz. An attractive application for our FMCW terahertz systems is the inspection of aircraft radomes during manufacturing and in field use. Aircraft radomes are strongly exposed to environmental conditions and may sustain impact damages from swirled up stones, hail, and bird strikes. Since the structures of these radomes are mostly constructed of GFRP-based composites similar to the example shown in Fig. 2c, the most established method for regular inspection is tap tests [17], which must be performed manually and provide only limited information. Furthermore, radomes are built layer by layer and an inline production

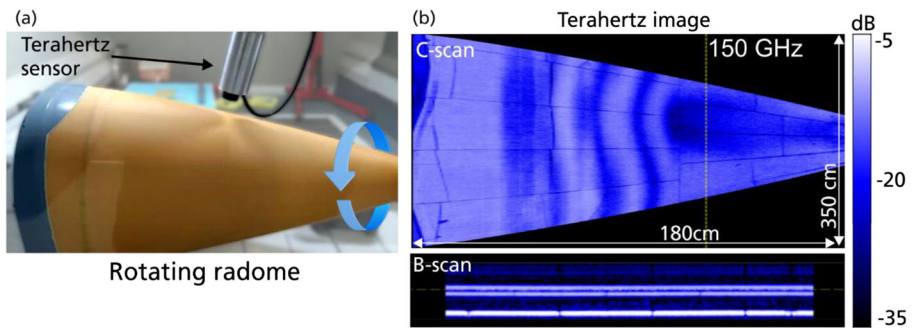


**Fig. 3** **a** A rotating multilayer composite radome is inspected with a terahertz sensor, which comprises two FMCW transceivers with collinear beam path. The system is integrated in the manufacturing environment of the radome. **b** Unwrapped terahertz image of the revealing individual composite panels in the C-scan (top) and multilayer structure in the B-scan (bottom) at the indicated position in the C-scan image

quality control can be realized to detect possible structural imperfections, delaminations, and other defects already during the manufacturing process [15]. Figure 3 depicts a dual-frequency FMCW imaging system, which we integrated into a production environment of aircraft radomes. In the present configuration, the terahertz sensor consists of two individual, all-electronic multiplier chain transceivers, one operating in the range between 70 and 110 GHz and the other working from 110 to 170 GHz. The two transceiver units are packaged within single sensor housing and their individual, linearly polarized beams are aligned collinearly with the help of a wire-grid polarizer. In this way, both transceivers are using the same quasi-optical setup and the measurement data can be acquired at the same position with both transceivers operating simultaneously and independently. The measurement sensor is attached to the tool holder of a robotic machining center, which is used for the construction process of the radomes. While the radome is spinning on a rotational stage along its center axis, the sensor moves along the surface to acquire terahertz images of the full radome structure along a spiral-shaped trajectory with adjustable pitch between roundtrips. Depth information for full three-dimensional volume images of the composite structure is recorded along this trace with the help of the FMCW measurement principle. Figure 3a shows a photograph of the FMCW terahertz sensor in operation during the inspection of an exemplary radome in production. Figure 3b displays the (unwrapped) image of a single depth layer roughly 5 mm below the surface of a full aircraft radome structure acquired with the 150 GHz transceiver unit of the sensor. The image reveals good spatial resolution of individual panels of the composition of the radome structure. Currently, we are working towards standardization of this nondestructive testing method together with the UK National Aeronautical NDT board.

### 2.3 Quality Control of Acoustic and Thermal Insulation

The high sensitivity of the terahertz measurement technique allows for the inspection of soft materials such as open-cell foam, which is widely used for thermal and acoustic insulation in boats, trains, automobiles, and aircrafts. Foam materials often contain hidden defects from the production process, such as voids within a larger volume. Standard X-ray techniques usually do not exhibit sufficient contrast for defect detection and application of a coupling medium required for ultrasound measurements is not easily possible. On the other hand, the capability to obtain depth information via the FMCW measurement principle in combination with

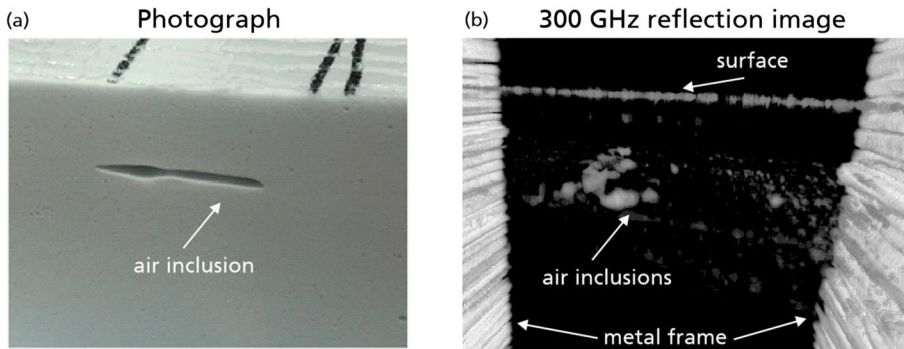


**Fig. 4** **a** Photograph of an air inclusion (height of  $\sim 5$  mm, length of  $\sim 5$  cm) roughly 2 cm below the surface of an open-cell foam. **b** 3D volume image recorded at around 300 GHz with air inclusions clearly visible throughout the sample

millimeter spatial resolution of terahertz radiation allows for an accurate three-dimensional localization of voids within such low-density foam materials.

The photograph in Fig. 4a on the left shows a typical void within a (cut-open) block of open-cell foam, while Fig. 4b depicts an exemplary volumetric image of a similar sample obtained in an FMCW terahertz measurement at around 300 GHz in reflection mode and measured from the top of the sample. The three-dimensional image shows a similar perspective as in the optical photograph (but showing data of a different, comparable block of open-cell foam). The strong signals on the left and right edges of the image stem from a metallic sample holder of the setup. Within the open-cell foam, a concentration of voids of different sizes can clearly be identified. The signatures appear roughly at the same depth below the surface as in the optical photograph, indicating that this is the typical location of flaws in the product and that the FMCW terahertz measurement system is able to detect and locate the defects.

The terahertz measurement shown in Fig. 4 was performed with a single transceiver unit in connection with x-y raster-scanning mechanics. In order to address industrial inline inspection, a fast-scanning axis in connection with a conveyor belt can be used to achieve feed motions of a few millimeters per second. An even faster approach for gathering volumetric images could be the use of sensor array configurations as described within the following section.

## 2.4 Inline Inspection with Sparse Arrays

The usage of millimeter wave and terahertz imaging systems for industrial inline inspections places high demands on image acquisition speed, scalability, cost-effectiveness, and detection sensitivity. Within the last decade, interesting approaches for millimeter wave and terahertz imaging systems with real-time capabilities were introduced (e.g., [18–20]). In most cases, these concepts are based on either full sensor (line) arrays or fast-scanning optics. While quasi-optical systems suffer limited lateral resolution within fixed focal distances, most system concepts with fully populated sensor arrays demand a trade-off between field of view and image resolution because of the limited array size. On the other hand, realization of a densely populated sensor array is often not feasible and the distribution of transceiver elements must be considered in detail regarding a specific application scenario. Here, the use of sparse arrays in combination with numerical focusing algorithms is an effective solution, which can overcome the above-mentioned limitations, however, at the cost of higher computational efforts. In the

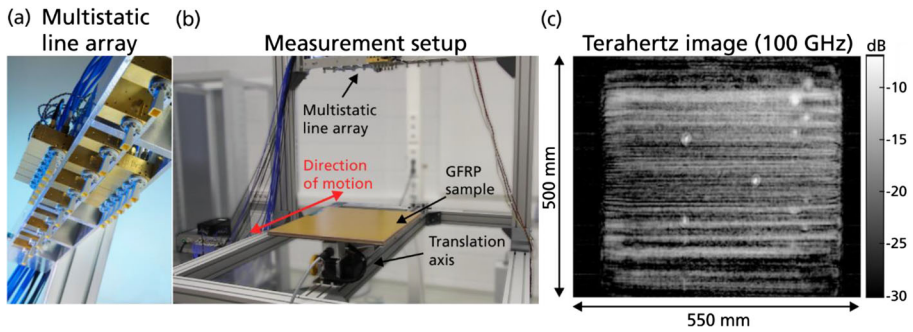


**Fig. 5** **a** Multistatic line array containing 12 transmitters and 12 heterodyne receivers. **b** Measurement setup with multistatic array and translation axis for terahertz imaging. **c** Terahertz image of GFRP sample acquired with line array (feed motion of 19.2 cm/s)

latter approach, the convolution of a sparse spatial distribution of terahertz transmitters and another sparse spatial distribution of terahertz receivers can form a full synthetic transceiver array. The photograph in Fig. 5a shows the realization of a terahertz measurement system following this concept, which was developed in our group. Some more details of our system are given in [21, 22]. The multistatic line array consists of 12 W-band transmitters (Tx) and 12 W-band heterodyne receivers (Rx). The array is mounted above a translation axis, which imitates the feed motion of a conveyor belt, as displayed in Fig. 5b. A synthetic aperture is created along the direction of motion, where we benefit from a stepped-frequency modulation covering a bandwidth of 35 GHz around 100 GHz center frequency.

A fast switching matrix is used to sequentially operate the emitters for each frequency point, while the receivers simultaneously record the received signals from the illuminated object. This approach allows volumetric imaging at feed motions of several 10 cm/s, depending on the amount of frequency points with an underlying frequency switching time of the system of 300  $\mu$ s. The implementation of fast image reconstruction algorithms in connection with parallel data processing on a graphics processing unit (GPU) provides real-time image reconstruction [22]. The image in Fig. 5c shows the inner layer of GFRP composite test sample (see photograph in Fig. 5b), which was recorded with a feed motion of the translation axis of 19.2 cm/s. The test sample was the same as was shown in the terahertz image in Fig. 2c. Again, the artificially implemented defects within the structure can be clearly seen in the image acquired with the line array measurement system. In contrast to the image in Fig. 2c, the image recorded with the array exhibits a significant line pattern due to a violation of the Nyquist-Shannon sampling theorem by the extreme sparsity of the array. The spatial sampling along the array axis can be controlled by the array design and can be customized for the requirements of a specific application.

## 2.5 Mobile Inspections

In order to address manual terahertz inspection for field-use, the FMCW transceiver concept (compare Fig. 2) was integrated into a mobile handheld device with an integrated linear position encoder. Figure 6a shows the handheld terahertz sensor together with a mobile PC for data acquisition and processing. A- and B-scans of an object under test are performed by moving the point sensor manually along the sample with the sensor placed on its surface on integrated wheels. Figure 6b shows an example of a line scan (B-scan) of a test sample made of

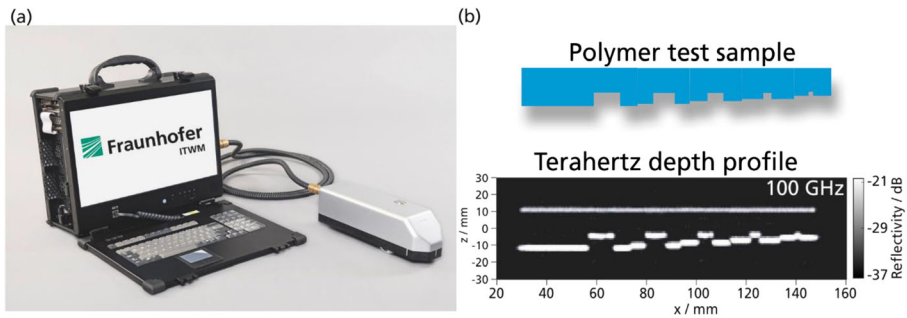


**Fig. 6** **a** Handheld FMCW terahertz sensor. **b** Example measurement at around 100 GHz of a polymer test sample with a flat surface and a structured back as shown in the top scheme. The structure can be clearly reproduced by moving the handheld along the flat surface

polyethylene with an overall wedge shape and flat bottom holes of different size and depth on the backside. The terahertz image is generated in real-time as the sensor moves along the sample and displayed continuously during the measurement. The implemented holes and steps in the test sample can be well identified in the terahertz depth profile image. With prior knowledge of the dielectric properties of a sample under test—for example, from additional terahertz test measurements on reference samples of known thickness—the FMCW measurement principle can provide absolute quantitative information on the thickness and shape of the investigated features. The next section addresses this topic in particular.

## 2.6 FMCW Thickness Measurements

While broadband terahertz systems based on the TDS measurement principle are widely employed for thickness inspections of thin dielectric multilayer structures—e.g., for paint layers, as highlighted in section 3—a strong signal attenuation, particularly in thick samples with several millimeters to centimeters of thickness, can limit the applicability of this technique. In the millimeter wave and lower terahertz regime, FMCW systems provide a high dynamic range of up to 70 dB at measurement rates of several kilohertz in connection with higher signal penetration depth than pulsed terahertz systems. Recently, we demonstrated the suitability of such systems for thickness measurements and proved that layer thicknesses even below the Rayleigh resolution limit can be resolved by taking advantage of a model-based signal processing technique [23, 24]. In a basic approach, modeled versions of the measurement signal are computed a priori based on estimated properties of the multilayer material system under test. The real measurement signal is then correlated with the individual signal models. The layer properties with the best agreement between signal model and measurement represent the final result. In this way, the minimum layer resolution of the measurement system can be improved significantly by proper consideration of the a priori information. Multiple reflections can be taken into account by using the transfer-matrix method for the calculations of the signal models [24].

In order to prove the feasibility of the approach, we compared the measurement results from a multilayer structure obtained with a broadband terahertz TDS system as a reference, and an FMCW terahertz system operating between 70 and 110 GHz [24]. Figure 7 shows the results of TDS and FMCW measurements along a three-layer tube wall, which consists of a dense recycle foam structure, sandwiched between two thin layers of polyvinyl chloride (PVC).

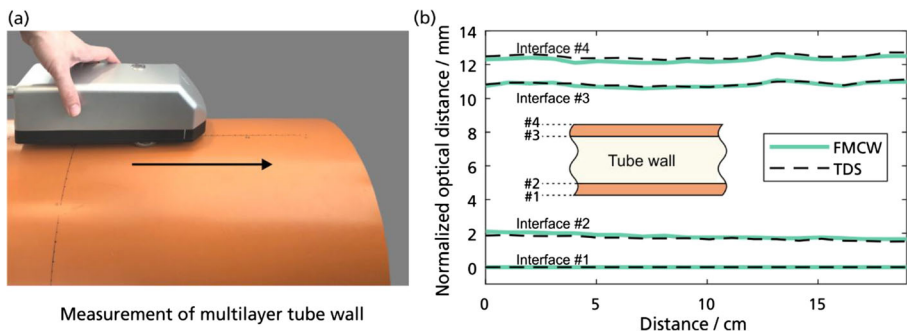


**Fig. 7** **a** Illustration of an FMCW measurement (90 GHz center frequency) of the layer thicknesses of a three-layer polymer tube wall along the indicated direction exploiting the signal modeling technique. **b** Comparison of optical distances (optical path lengths) of the four interfaces of the tube's layer structure measured with a terahertz TDS system (dashed lines) and the shown handheld FMCW system (solid green lines). The data is referenced to the first (outer) interface at 0 mm

The TDS measurements of the tube wall (shown as dashed lines in Fig. 7c) yield an optical thickness of around 8.8 mm for the foam layer and optical thicknesses of 1.95 mm and 1.5 mm for the outer and inner PVC layers, respectively. In contrast, the FMCW system with 40 GHz frequency modulation bandwidth has a theoretical thickness resolution limit of 3.75 mm (compare Eq. (2)). Hence, the inner and outer layers are well below the inherent resolution limit of the system. However, the FMCW measurement technique in combination with the signal modeling approach described above achieves a thickness resolution, which compares well with the TDS measurements on the same multilayer material system. Therefore, FMCW thickness measurements in combination with proper signal processing can serve as a powerful complementary technique for thickness measurements in material systems at high measurement rates where strong signal attenuation prevents the use of standard TDS systems.

### 3 Submillimeter Layer Characterization

In many industrial applications, the quality of thin layers has to be assured, which is increasing the demand on the presented nondestructive measurement techniques. Besides the already-presented electronic terahertz approach, the TDS technique provides a further access to the terahertz frequency range [25]. This technique uses ultrashort laser pulses to generate short terahertz pulses, which are then sampled in the time domain by using delayed laser pulses and a detector, which is only active for a sub-picosecond time window. By varying the delay between the laser pulses, the terahertz waveform is sampled, providing a phase-sensitive measurement method. Modern state-of-the-art TDS systems for industrial applications provide dynamic ranges of more than 60 dB and a frequency range from below 100 GHz to above 4 THz at a measurement time of 1 s [26, 27]. Due to their higher terahertz frequency in comparison with electronic systems, these systems are often used for characterizing submillimeter layers down to and even below 10  $\mu\text{m}$  absolute thickness [28]. Interestingly, the evaluation of layer thicknesses is possible also for sub-wavelength layers, for example by applying retrieval algorithms [29–32]. Figure 8 illustrates the analogy of time-domain and frequency-domain signals of thick and thin single-layer measurements.

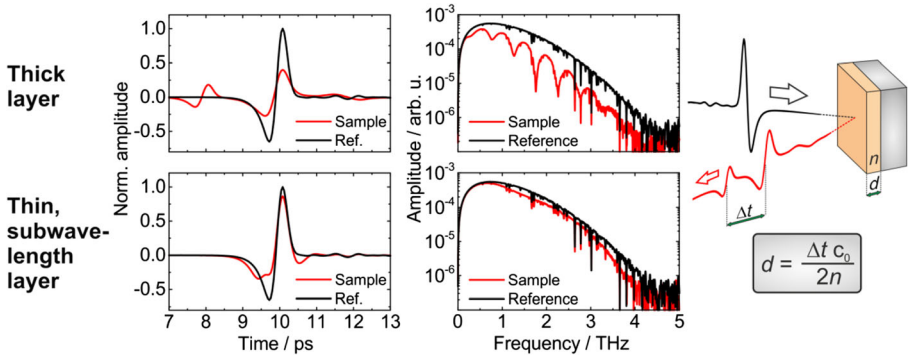


**Fig. 8** Difference of the time-domain and frequency-domain response of thick and thin sub-wavelength layers in reflective terahertz measurements. In both domains, the layer thickness information is contained and can be extracted. For thin layers, the time-domain data do not provide separable pulses and no directly extractable minima in the frequency domain, but still enable the extraction of layer thickness when applying retrieval algorithms

The evaluation principle of time-domain data of layer thickness measurements often bases on retrieval algorithms (see Fig. 9), as simple methods (such as peak-finding) are only applicable, if thick layers are considered. For thin, sub-wavelength layers (less than the mean wavelength of about 150 μm), the individual peaks caused by the adjacent interfaces of a layer structure are not distinguishable anymore. Therefore, model-based retrieval algorithms have to be used to extract the layer thickness information. For this, a reference measurement has to be taken in advance. With this reference measurement and the sample measurement, the algorithm bases on varying the transfer function and applying it to the reference measurement until the best match between sample measurement and simulation is found. The optimization algorithm used in this evaluation process is crucial for the performance and computational efficiency of this principle. Modern algorithms enable the evaluation of multilayer measurements within less than a millisecond on standard CPUs.

This evaluation principle is not only applicable to extract the layer thickness, but also to determine the unknown optical constants and the layer thicknesses at the same time [33, 34]. Figure 10 shows the evolution of these constants (or variables in this case) during a run of the

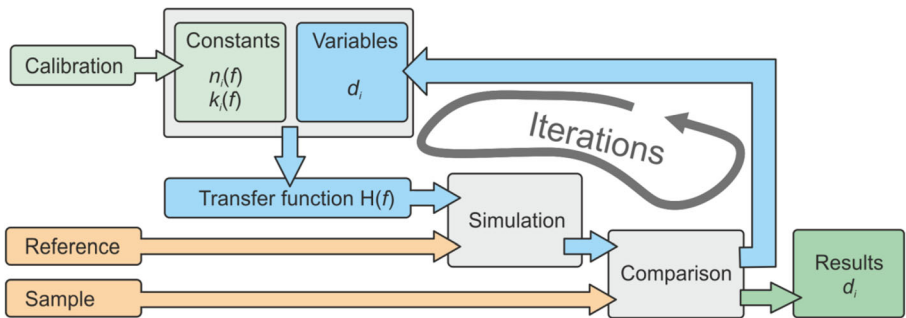


**Fig. 9** Schematic of the evaluation algorithm. The reference measurement is used to simulate a measurement result and compare it with the real sample measurement. If the comparison results in a bad correlation, the simulation is carried out again with optimized variables. The used constants are taken from an earlier process of calibration. Once the comparison gives a sufficient correlation of simulation data and sample measurement, the results are returned

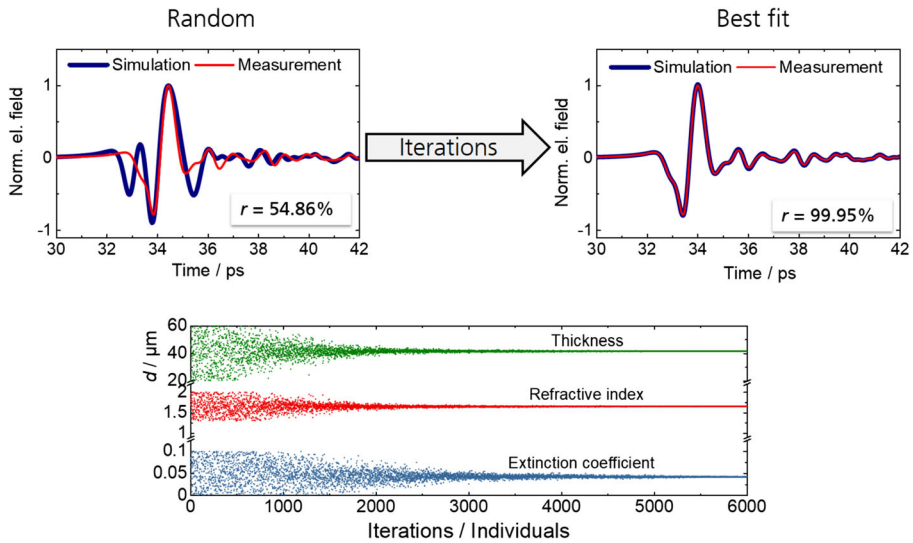


**Fig. 10** Example of an evaluation process, where thickness, refractive index, and extinction are determined simultaneously. Starting with a simulation using random parameters, the algorithm finds the best fit over a large number of iterations and individuals. This principle cannot only be applied to find the thickness value, but also to find refractive index, extinction coefficient, and thickness. This method works best for a low number of layers

optimization algorithm finding the thickness, refractive index, and extinction coefficient of a single-layer coating. Starting with a random set of variables, the simulation is carried out over and over again varying the three variables until a best fit is found that reproduces the measurement. This method is suitable for a limited set of layers, as the optimization routines become unstable for a higher number of variables.

### 3.1 Thickness Determination of Painted Car Bodies for the Automotive Industries

One of the most prominent industrial applications of terahertz TDS systems is the measurement of individual layer thicknesses in a multilayer structure of coatings, e.g. of car bodies [30, 35–42]. Compared with already-established techniques, terahertz technology offers unique advantages as the capability of measuring nondestructively and contactless. Figure 11 presents

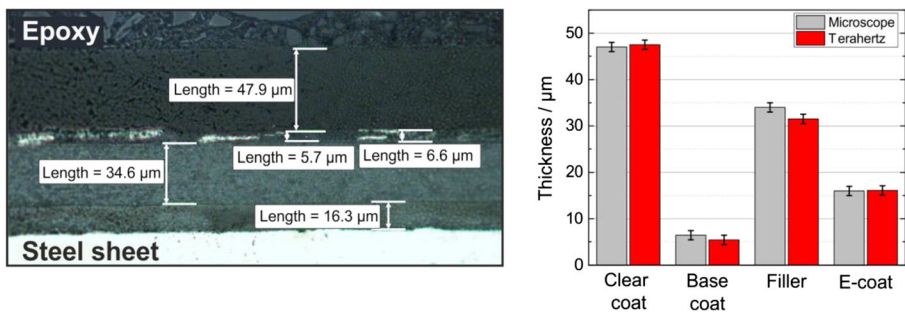


**Fig. 11** Cross section of a typical four-layer coating on a steel sheet used in the automotive industries. The covering epoxy layer is only used for creating the cross section. The terahertz results meet the microscopy values within the given accuracy, which also depends on the location of the cross section as well as the evaluation principle of the microscope image

a cross-section microscopy image along with the results from the terahertz layer-thickness determination. The cross-section method is often used as a “golden standard,” even though this technique also underlays uncertainties, as the location of the cross section and the location of the microscopic investigation influence the result—this should always be taken into account. Nevertheless, the results from the terahertz layer-thickness determination of the four-layer coating depicted in Fig. 11 agree well with the microscopy values.

Nowadays, not all car body parts are based on metal, but also on plastics, especially crash-relevant structures, which should return to their original form after minor crashes (bumpers etc.). As these structures shall look identical to the rest of the car body for design reasons, they are coated with multilayer structures as well. As long as the refractive index contrast is sufficient, terahertz technology is able to determine these layer thicknesses as well, as it does not depend on a metallic substrate. Coatings on composite materials such as GFRP or CFRP (carbon fiber–reinforced plastics) can also be determined [43, 44], which is of growing interest, as modern vehicles often contain these materials.

### 3.2 Intermediate Devices—Thick and Thin at the Same Time

When applying terahertz techniques to layer thickness measurement tasks, the range of measurable thicknesses depends on the phase stability and dynamic range and most intuitively also on the accessible frequency or wavelength range. As TDS systems in general provide information in the frequency range from about 100 GHz to several terahertz, these systems can be used to measure moderately thick to some microns thin layers. The upper limit of this range is further defined by the material absorption and the system’s accessible delay range. Most commonly, a fast-scan delay range of about 100 ps is realized in classical TDS systems. Considering a refractive index of about 1.5, this results in an upper limit of about 10 mm measurable sample thickness using standard TDS systems in reflection. Modern approaches enable the measurement of much larger delay ranges but have not been demonstrated in automotive or aviation industries tasks yet [45, 46]. In some cases, the simultaneous measurement of thick and thin layers is of interest, which then can be carried out by using the TDS approach [47]. One example is shown in Fig. 12, where the measurement of a fuel tank wall is presented along with a schematic drawing of the layer structure. Fuel tanks are often multilayer structures, providing the resistance of the wall to the fuel content on the inside as well as the resistance to environmental influences on the outside. The example shown is a fuel tank wall consisting of two dielectric layers with a layer of glue in between. The time-domain data directly reveals this three-layer system.

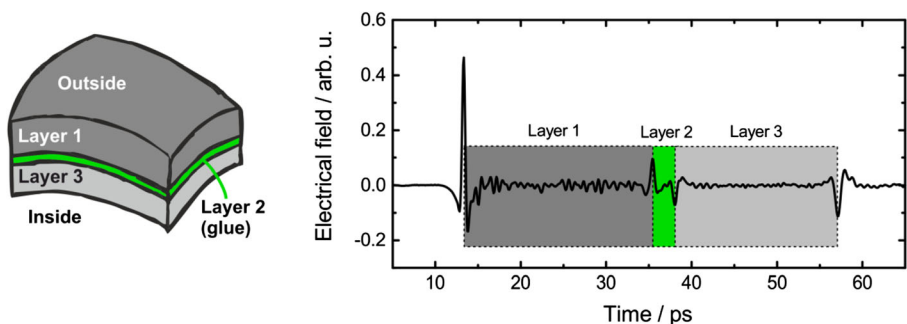


**Fig. 12** Schematic of a fuel tank wall, which is in this case a two-layer compound with a thin glue layer in between. In the time-domain data (right), all layers—thick and thin ones—can be identified properly

### 3.3 Wet Paint

Despite the advantage of nondestructively measuring product quality after the manufacturing and refining process, the inline measurement of these properties is most helpful to the manufacturer. This poses new challenges for the measurement equipment as the need for measurement speed, robustness, and especially for the paint layer thickness measurement new material properties have to be taken into account. In paint processes, it is of highest interest to recognize deviations from the desired process during the process itself. So the measurement of wet paint has to be enabled to provide the manufacturer the most useful information to the earliest possible time. In the wet state, it is often better to add additional paint for thickness correction in comparison to do so after the first curing, not to generate a boundary in between which influences the optical appearance of the product and its mechanical properties. In addition to that, the cycle time for inspection and production is reduced. In general, there are two categories that have to be taken into account, when considering the measurement of wet paint: solvent-based and water-based paint. As the alcohol-based solvents are showing considerably different optical properties in comparison with the strongly absorbing bulk water, these two classes behave differently in the terahertz frequency range. Even though the absorption of bulk water is very high in the terahertz frequency range (about  $250\text{ cm}^{-1}$  at 1 THz), the measurement of water-based paint is possible in general, as the layer thickness of wet paint is often less than a millimeter [33, 34, 48, 49].

Figure 13 shows a measurement of wet paintings on a metallic substrate directly after the application of the paint and after curing in comparison with a tactile measurement with an inductive sensor. These measurements show the shrinking behavior of the wet coatings and the good

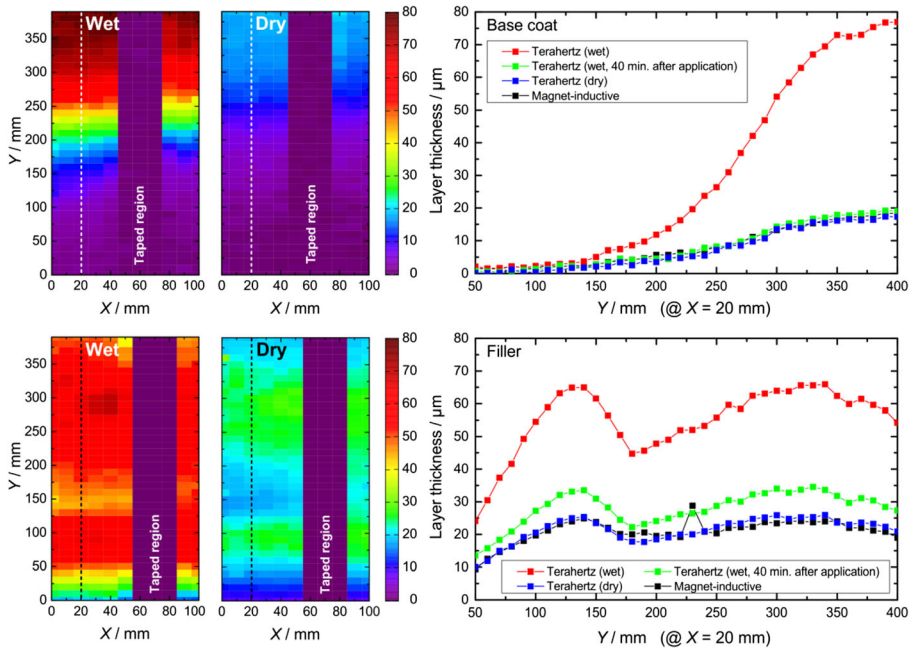


**Fig. 13** Measurement examples of measuring wet paint layers. Plane substrates were painted with base coat or filler coat, respectively. After the application, 2D images were acquired with a TDS system immediately after the application of the paint as well as during and after drying of the paint. A good agreement with a magnet-inductive sensor as well as the reasonable drying behavior (conserving the overall spatial distribution) demonstrates the applicability of terahertz sensors to measure wet paintings

agreement between terahertz measurements of the dry paint state and inductive measurements. The shrinking factor of the base coat and filler is about 4 and 2.5, respectively. Obviously, the magnet-inductive measurement is not able to measure the wet state of the coatings, as the mechanical contact would strongly influence the measurement value and could lead to destruction of the coating surface.

### 3.4 Measuring Safety-Relevant Features of Car Interiors

Not only paint processes can be nondestructively monitored with the help of terahertz technology. There are much more applications in the automotive industry where this technology can provide a benefit [3]. The interior of automobiles, for example, is of high interest, as it is the interface to the customer. Therefore, the design should not be disturbed by features needed for functionality but only be defined by the design rules. In modern cars, there are plenty of safety features, with the most prominent being the airbags. Airbags are often hidden behind the surface of the steering wheel or the panel in front of the passengers. These panels have very small perforations on the backside that hide the airbag, but enable the inflation of it in the case of a crash. These perforations are very critical not to be too coarse—it should be invisible to not influence the design—and not too sparse, as this would hinder the efficient and fast inflation. The panel material is called “slush skin” and can be checked using terahertz waves. Terahertz TDS measurements of perforations in a slush skin are presented in Fig. 14. The intensity plot reveals the location of the perforation and the time-domain data allow for an estimation of the perforation depth.

Due to the small hole size of the perforation, the depth estimation accuracy is limited, which could be enhanced by different optical setups. Further, as the surface and the interior structure of the slush skin are not flat and homogeneous, this application is challenging, as the terahertz waves get scattered. Different improvements, e.g., by using other terahertz optics, are in development to enhance the data quality, but the presented results already prove the feasibility of this application.

### 3.5 Aspects of Real-world Application in Production Environment

When using terahertz technology and especially the TDS principle in the automotive industry, one has to adapt to the conditions present there. Often, the testing should be performed close to

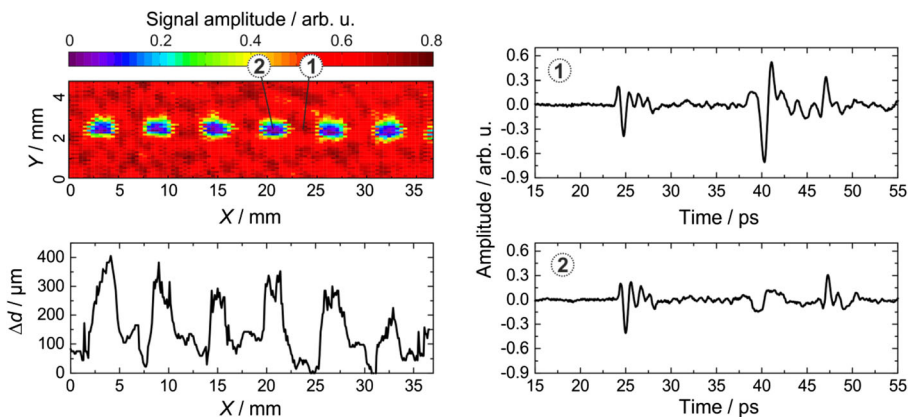


**Fig. 14** Time-domain 2D imaging of the perforation in a slush skin of a car interior, estimated thickness, and two waveforms at different points on the sample. The perforation is considered to enable the efficient and fast inflation of an airbag in the case of a crash. Even though the perforation holes are very thin, their depth can be estimated using terahertz technology

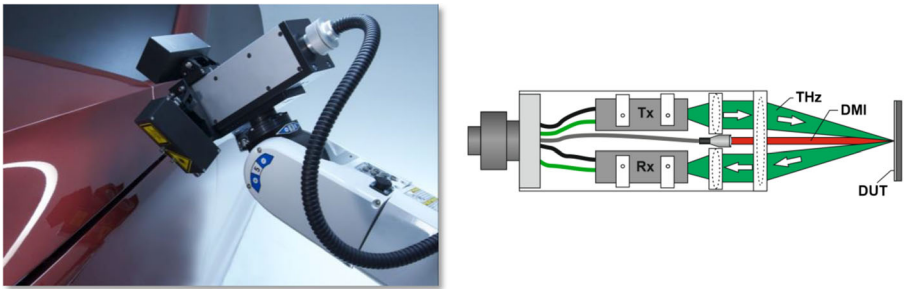


**Fig. 15** (Left) Terahertz sensor mounted on a robot during the measurement of individual layer thicknesses of a multilayer painting on a car body. (Right) Schematic setup of a pitch-catch terahertz transceiver with an integrated displacement-measuring interferometer sensor for vibration compensation

the place of manufacturing, which often implies the influences of a harsh environment. The usability of robotic systems to bring the sensor to the device under test has been proven in the past [3, 50]. The application of robots and the rough environment lead to the need of insensitivity to vibrations [51, 52]. They can lead to severe disturbance of the acquired terahertz signal—especially when applying the most common TDS principle.

By combining a high-speed displacement-measuring interferometer (DMI) with the TDS system, this limitation can be overcome. The DMI measures the distance of the sensor head to the device under test with a rate of more than 1 MHz and enables the correction of the acquired terahertz data, so that the influence of the vibration can be wiped out. Figure 15 depicts a photograph of a terahertz transceiver mounted on a robot for measuring car body paints and the schematic setup of it. The integration of the DMI is realized by using a terahertz pitch-catch setup and a collinear DMI beam. The measurements of two-layer structures which were disturbed by induced vibrations are presented in Fig. 16.

Depending on the product of amplitude and frequency of the vibration, a deviation of the extracted layer thickness is induced. This deviation strongly depends on the layer structure and increases with the number of layers. Using the DMI information, the layer thickness determination accuracy can greatly be enhanced, which results in a vanishing deviation. This technique enables the employment of terahertz TDS technology in a rough industrial environment.

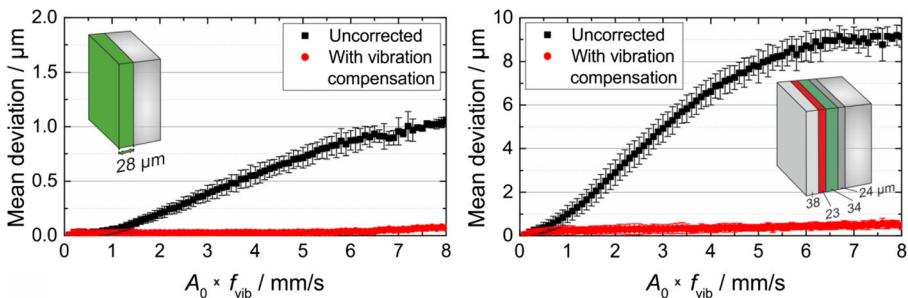


**Fig. 16** Influence of vibrations onto the result of layer thickness measurements on two different samples. The deviation from the real value increases drastically with increasing amplitude  $A_0$  or frequency  $f_{vib}$  of the sample’s vibration. When using a displacement-measuring interferometer, the unfavorable influence of the vibration can be almost fully suppressed. The influence of vibrations is much higher on multilayer coatings, if no compensation techniques are used

## 4 Conclusions and Outlook

In this contribution, we have shown that terahertz technology is a very useful tool in the field of nondestructive testing. The presented results of measurements on samples from automotive and aviation industries give a proof that quality inspection with this new upcoming technology is very attractive and no longer only working under laboratory conditions. The step out of the lab into industries depending on the specific application is either in progress or has already been done as shown for the vibration compensation method for multilayer paint systems.

Enhancing the scanning frequency of TDS systems is a demand that is very often discussed especially in terms of industrial use to either realize a rapid 2D scanning or to observe fast single processes. The limitations in classical systems to less than 100 Hz of pulse acquisition rate are mainly determined by the mechanical delay line. It has been shown that a smart timing management of two femtosecond lasers—known as asynchronous optical sampling (ASOPS)—could lead to pulse repetition rates in the kilohertz regime. Further improvements basing on this principle are named electronically controlled optical sampling (ECOPS) [45] and single-laser polarization-controlled optical sampling (SLAPCOPS) [46]. Both methods have the advantage to flexibly change the scanning range to match the region of interest and not to waste measurement time. Here, SLAPCOPS is potentially more cost-effective as only one laser is needed using its different polarization states in the fiber instead of two single-laser systems. It should be noted that the dynamic range is only depending on the measurement acquisition time so fast-scanning delay lines need the same time to achieve the same dynamic range.

Another demand which has been coming up with the birth of the first terahertz systems is the reduction of the systems costs. As already mentioned, the main cost-driving device of a TDS system is the femtosecond laser system. Hence, there are efforts to get rid of the pulsed femtosecond laser sources by introducing multimode diode lasers [53] or as most recently demonstrated superluminescent diodes [54]. Up to now, these systems supply a lower performance but in principle similar signals compared with standard TDS that might be sufficient for specific applications with moderate demands.

Future electronic terahertz systems profit from the tremendous development of millimeter-wave and terahertz-integrated circuits, which can provide a significant cost reduction and allow for more compact system designs as well as highly integrated multistatic array solutions such as shown for microwave imaging in [55]. Besides stepped-frequency and FMCW radar approaches [56–58], also broadband pulsed systems can be considered [59].

**Open Access** This article is licensed under a Creative Commons Attribution 4.0 International License, which permits use, sharing, adaptation, distribution and reproduction in any medium or format, as long as you give appropriate credit to the original author(s) and the source, provide a link to the Creative Commons licence, and indicate if changes were made. The images or other third party material in this article are included in the article's Creative Commons licence, unless indicated otherwise in a credit line to the material. If material is not included in the article's Creative Commons licence and your intended use is not permitted by statutory regulation or exceeds the permitted use, you will need to obtain permission directly from the copyright holder. To view a copy of this licence, visit <http://creativecommons.org/licenses/by/4.0/>.

## References

1. D. Zimdars, J. S. White, G. Stuk, A. Chernovsky, G. Fichter, and S. Williamson, “Large area terahertz imaging and non-destructive evaluation applications”, *Insight - Non-Destructive Testing and Condition Monitoring*, Volume 48, Number 9, 1st September 2006, pp. 537–539(3)

2. M. Tonouchi, “Cutting-edge terahertz technology”, *Nature Photonics* volume 1, pages 97–105 (2007)
3. C. Jansen, S. Wietzke, M. Scheller, N. Krumbholz, C. Jördens, K. Baaske, T. Hochrein, M. Koch, and R. Wilk, “Applications for THz Systems”, *Optik & Photonik*, (2008)
4. Y.-C. Shen, and P. F. Taday, “Development and Application of Terahertz Pulsed Imaging for Nondestructive Inspection of Pharmaceutical Tablet”, *IEEE Journal of Selected Topics in Quantum Electronics* (Volume: 14, Issue: 2, March-April 2008)
5. I. Duling, and D. Zimdars, “Revealing hidden defects”, *Nature Photonics* volume 3, pages 630–632 (2009)
6. S. Wietzke, C. Jansen, C. Jördens, N. Krumbholz, N. Vieweg, M. Scheller, M. K. Shakfa, D. Romeike, T. Hochrein, M. Mikulics, and M. Koch, “Industrial applications of THz systems”, *Proc. SPIE 7385, International Symposium on Photoelectronic Detection and Imaging 2009: Terahertz and High Energy Radiation Detection Technologies and Applications*, 738506 (4 August 2009) <https://doi.org/10.1117/12.840991>
7. F. Ospald, W. Zouaghi, R. Beigang, C. Matheis, J. Jonuscheit, B. Recur, J.-P. Guillet, P. Mounaix, W. Vleugels, P. V. Bosom, L. V. Gonzalez, I. Lopez, R. M. Edo, Y. Sternberg, and M. Vandewal, “Aeronautics composite material inspection with a terahertz time-domain spectroscopy system”, *Optical Engineering*, 53(3), 031208 (2013) <https://doi.org/10.1117/1.OE.53.3.031208>
8. I. Amenabar, F. Lopez, and A. Mendikute, “In Introductory Review to THz Non-Destructive Testing of Composite Mater”, *J. Infrared Milli. Terahz. Waves* (2013) 34: 152 <https://doi.org/10.1007/s10762-012-9949-z>
9. TEMATYS SARL, “Terahertz Components & Systems: Technology and Market trends UPDATE 2016”, July 2016
10. F. Ellrich, J. Klier, S. Weber, D. Molter, J. Jonuscheit, and G. von Freymann, “Terahertz thickness determination for industrial applications: Challenges and solutions”, [keynote], *SPIE - Photonics West* [10531–23], San Francisco, CA, USA, January 30th, 2018
11. “Development and Optimization of THz NDT on Aeronautics Composite Multi-layered Structure”, Public EU project DOTNAC, Grant ID: 266320, <https://cordis.europa.eu/project/rcn/96573/factsheet/en>, Accessed 07 June 2019.
12. E. Cristofani, F. Friederich, S. Wohnsiedler, C. Matheis, J. Jonuscheit, M. Vandewal, and R. Beigang, “Nondestructive testing potential evaluation of a terahertz frequency-modulated continuous-wave imager for composite materials inspection.” *Opt. Eng.*, 53, 031211 (2014) <https://doi.org/10.1117/1.OE.53.3.031211>
13. E. Cristofani, F. Friederich, M. Vandewal, and J. Jonuscheit, “Advanced Ultrawideband Radar” by James D. Taylor, Chapter on “Non-destructive testing of aeronautics composite structures using UWB radars”, CRC Press, 2017.
14. F. Friederich, E. Cristofani, C. Matheis, J. Jonuscheit, R. Beigang, and M. Vandewal, “Continuous wave terahertz inspection of glass fiber reinforced plastics with semi-automatic 3-D image processing for enhanced defect detection”, *IEEE MTT-S International Microwave Symposium* (2014), <https://doi.org/10.1109/MWSYM.2014.6848486>
15. F. Friederich, K.H. May, B. Baccouche, C. Matheis, M. Bauer, J. Jonuscheit, M. Moor, D. Denman, J. Bramble, and N. Savage, “Terahertz Radome Inspection”, *Photonics*, vol. 5(1), 1, (2018) <https://doi.org/10.3390/photonics5010001>
16. S. Heuel, T. Koepfel, and S. Ahmed “Evaluating 77 to 79 GHz Automotive Radar Radome Emblems”, *Microwave Journal*, 61(1), pp. 70–78 (2018)
17. R.H. Bossi and V. Giurgiutiu, “Nondestructive testing of damage in aerospace composites”, In: *Polymer Composites in the Aerospace Industry*, pp. 413–448 (2015), <https://doi.org/10.1016/b978-0-85709-523-7.00015-3>
18. F. Friederich, W. von Spiegel, M. Bauer, F. Meng, M.D. Thomson, S. Boppel, A. Lisauskas, B. Hils, V. Krozer, A. Keil, T. Löffler, R. Henneberger, A.K. Huhn, G. Spickermann, P. Haring Bolívar, and H.G. Roskos, “THz active imaging systems with real-time capabilities”, *Inaugural issue of IEEE Trans. Terahertz Sci. Technol.*, 1, pp. 183–200 (2011), <https://doi.org/10.1109/TTHZ.2011.2159559>
19. S. S. Ahmed, A. Schiessl and L. Schmidt, “A Novel Fully Electronic Active Real-Time Imager Based on a Planar Multistatic Sparse Array”, *IEEE Trans. Microwave Theory Tech.*, 59(12), pp. 3567–3576 (2011), <https://doi.org/10.1109/TMTT.2011.2172812>
20. J. Oden, J. Meilhan, J. Lalanne-Dera, J.-F. Roux, F. Garet, J.-L. Coutaz, and F. Simoens, “Imaging of broadband terahertz beams using an array of antenna-coupled microbolometers operating at room temperature”, *Opt. Express*, 21, pp. 4817–4825 (2013).
21. B. Baccouche, A. Keil, M. Kahl, P. Haring Bolívar, T. Löffler, J. Jonuscheit, and F. Friederich, “A Sparse Array Based sub-Terahertz Imaging System for Volume Inspection”, *European Microwave Conference*, Paris, 2015, pp. 438–441 <https://doi.org/10.1109/EuMC.2015.7345794>
22. B. Baccouche, P. Agostini, S. Mohammadzadeh, M. Kahl, C. Weisenstein, J. Jonuscheit, A. Keil, T. Löffler, W. Sauer-Greff, and R. Urbansky, P. Haring Bolívar and F. Friederich, “3D Terahertz Imaging with Sparse

- Multistatic Line Arrays”, *IEEE J. Sel. Top. Quantum Electron.*, 23(4), pp. 1–11 (2017), <https://doi.org/10.1109/JSTQE.2017.2673552>
23. N. S. Schreiner, B. Baccouche, W. Sauer-Greff, R. Urbansky, and F. Friederich, High-Resolution FMCW Terahertz Thickness Measurements, 47<sup>th</sup> European Microwave Conference (EuMC), 2017, pp. 1187–1190, <https://doi.org/10.23919/EuMC.2017.8231061>
  24. N. S. Schreiner, W. Sauer-Greff, R. Urbansky and F. Friederich, Multilayer Thickness Measurements below the Rayleigh Limit Using FMCW Millimeter and Terahertz Waves”, *Sensors*, 19(18), 3910 (2019), <https://doi.org/10.3390/s19183910>
  25. D. Grischkowsky, S. Keiding, M. Van Exter, and C. Fattinger, “Far-infrared time-domain spectroscopy with terahertz beams of dielectrics and semiconductors”, *JOSA B*, 7(10), pp. 2006–2015 (1990).
  26. F. Ellrich, T. Weinland, D. Molter, J. Jonuscheit, and R. Beigang, “Compact fiber-coupled terahertz spectroscopy system pumped at 800 nm wavelength”, *Rev. Sci. Instrum.* 82, pp. 053102, (2011)
  27. B. Sartorius, H. Roehle, H. Künzel, J. Böttcher, M. Schlak, D. Stanze, H. Venghaus, and M. Schell, “All-fiber terahertz time-domain spectrometer operating at 1.5  $\mu\text{m}$  telecom wavelengths,” *Opt. Express*, 16(13), pp. 9565–9570 (2008)
  28. T. Iwata, H. Uemura, Y. Mizutani, and T. Yasui, “Double-modulation reflection-type terahertz ellipsometer for measuring the thickness of a thin paint coating”, *Opt. Express* 22(17), pp. 20595–20606 (2014)
  29. S. Krimi, G. Torosyan, and R. Beigang, “Advanced GPU-based terahertz Approach for in-line multilayer thickness measurements,” *IEEE J. Sel. Top. Quantum Electron.* 23(4), pp. 1–12 (2017)
  30. S. Krimi, J. Klier, J. Jonuscheit, G. von Freymann, R. Urbansky, and R. Beigang, “Highly accurate thickness measurement of multi-layered automotive paints using terahertz technology”, *Appl. Phys. Lett.* 109(2), p. 021105, 2016
  31. J. Dong, A. Locquet, M. Melis, and D. S. Citrin, “Global mapping of stratigraphy of an old-master painting using sparsity-based terahertz reflectometry”, *Scientific Reports*, 7:15098, DOI:<https://doi.org/10.1038/s41598-017-15069-2>, 2017
  32. T. Yasuda, T. Iwata, T. Araki, and T. Yasui, “Improvement of minimum paint film thickness for THz paint meters by multiple-regression analysis”, *Appl. Opt.* 46(30), pp. 7518–7526 (2007)
  33. S. Weber, J. Klier, F. Ellrich, S. Paustian, N. Güttler, O. Tiedje, J. Jonuscheit, and G. von Freymann, “Thickness determination of wet coatings using self-calibration method”, *The 42nd International Conference on Infrared, Millimeter, and Terahertz Waves (IRMMW-THz)* (2017)
  34. F. Ellrich, J. Klier, S. Weber, J. Jonuscheit, and G. von Freymann, “Thickness determination of wet coatings using self-calibration method”, *SPIE - Photonics West* (2017)
  35. I. S. Gregory, R. K. May, K. Su, and J. A. Zeitler, “Terahertz car paint thickness sensor: Out of the lab and into the factory” *Infrared, Millimeter, and Terahertz waves (IRMMW-THz)*, 2014 39th International Conference on (2014)
  36. K. Su, Y.-C. Shen, and J. A. Zeitler, “Terahertz sensor for non-contact thickness and quality measurement of automobile paints of varying complexity” *IEEE Transactions on Terahertz Science and Technology*, 4(4), pp. 432–439, (2014)
  37. D van Mechelen, “An Industrial THz Killer Application?”, arXiv:1511.02464 (2015)
  38. I. S. Gregory, R. K. May, P. F. Taday, P. Mounaix, “Extending terahertz paint thickness measurements to advanced industry-standard automotive paint structures”, 41st International Conference on Infrared, Millimeter, and Terahertz Waves (IRMMW-THz) (2016)
  39. A. I. Hernandez-Serrano, E. Castro-Camus, “Determination of automobile paint thickness using non-contact THz-TDS technique”, 40th International Conference on Infrared, Millimeter, and Terahertz waves (IRMMW-THz) (2015)
  40. S. Krimi and R. Beigang, “Terahertz thickness measurements for real industrial applications: from automotive paints to aerospace industry”, *Proc. SPIE* 10103, Terahertz, RF, Millimeter, and Submillimeter-Wave Technology and Applications X, 101030U (2017)
  41. Y. Dong, J. Zhang, Y. Shen, K. Su, J. A. Zeitler, Non-destructive characterization of automobile car paints using terahertz pulsed imaging and infrared optical coherence tomography”, 40th International Conference on Infrared, Millimeter, and Terahertz waves (IRMMW-THz) (2015)
  42. M. Picot, H. Ballacey, JP. Guillet, Q. Cassarand P. Mounaix, “Terahertz Paint Thickness Measurements: from lab to automotive and aeronautics industry”, 15th Asia Pacific Conference for Non-Destructive Testing (APCNDT2017) (2017)
  43. F. Ellrich, M. Theuer, D. Molter, M. Kannengießner, J. Jonuscheit, and R. Beigang, “Industrial Application of Terahertz Imaging: Non-Destructive Inspection of Thin Films and Ceramics”, *International Workshop on Terahertz Technology*, Osaka University Nakanoshima Center, Osaka, Japan, 30th November - 3rd December 2009
  44. K. H. Im et al., “Coating Thickness Characterization of Composite Materials Using Terahertz Waves”, *Materials Science Forum*, Vol. 878, pp. 70–73, 2017

45. M. Yahyapour, A. Jahn, K. Dutzi, T. Puppe, P. Leisching, B. Schmauss, N. Vieweg, A. Deninger, “Fastest Thickness Measurements with a Terahertz Time-Domain System based on Electronically Controlled Optical Sampling”, *Appl. Sciences* 9(7), 1283 (2019)
46. M. Kolano, B. Gräf, S. Weber, D. Molter, and G. von Freymann, “Single-laser polarization-controlled optical sampling system for THz-TDS”, *Opt. Lett.* 43(6), pp. 1351–1354 (2018)
47. J. Jonuscheit, “Terahertz Waves for Thickness Analyses: Non-destructive component analysis using terahertz time domain spectroscopy”, *Optik & Photonik*, 2016
48. T. Yasui, T. Yasuda, K. Sawanaka, T. Araki, “Terahertz paintmeter for noncontact monitoring of thickness and drying progress in paint film”, *Appl. Opt.* 44, 6849 (2005)
49. J. L. M. van Mechelen, “Predicting the dry thickness of a wet paint layer”, 43rd International Conference on Infrared, Millimeter, and Terahertz Waves (IRMMW-THz) (2018)
50. E.-M. Stübling, A. Rehn, T. Siebrecht, Y. Bauckhage, L. Ohrström, P. Eppenberger, J. C. Balzer, F. Rühli, and M. Koch, Application of a robotic THz imaging system for sub-surface analysis of ancient human remains”, *Sci. Rep.* 9, 3390 (2019)
51. T. Pfeiffer, S. Weber, J. Klier, S. Bachtler, D. Molter, J. Jonuscheit, and G. von Freymann, “Terahertz thickness determination with interferometric vibration correction for industrial applications”, *Opt. Express* 26(10), pp. 12558–12568 (2018)
52. D. Molter, M. Trierweiler, F. Ellrich, J. Jonuscheit, and G. von Freymann, Interferometry-aided terahertz time-domain spectroscopy”, *Opt. Express* 25(7), pp. 7547–7558 (2017)
53. A. Rehn, M. Mikerov, S. Preu, M. Koch, and J. C. Balzer, “Enhancing the performance of THz quasi time-domain spectroscopy systems by low duty cycle laser operation,” *Opt. Express* 26(25), 32758–32764 (2018)
54. D. Molter, M. Kolano, and G. von Freymann, Terahertz cross-correlation spectroscopy driven by incoherent light from a superluminescent diode“, *Opt. Express* 27(9), pp. 12659–12665 (2019)
55. S. S. Ahmed, A. Schiessl, F. Gumbmann, M. Tiebout, S. Methfessel and L. Schmidt, “Advanced Microwave Imaging”, in *IEEE Microwave Magazine*, vol. 13, no. 6, pp. 26–43, Sept.–Oct. (2012), <https://doi.org/10.1109/MMM.2012.2205772>
56. N. Pohl, T. Jaeschke, K. Aufinger, “An ultra-wideband 80 GHz FMCW radar system using a SiGe bipolar transceiver chip stabilized by a fractional-N PLL synthesizer”, *IEEE Trans. Microwave Theory Tech.* 60(3), pp. 757–765 (2012)
57. S. Scherr, B. Göttel, S. Ayhan, A. Bhutani, M. Pauli, W. Winkler, J.C. Scheytt and T. Zwick, “Miniaturized 122 GHz ISM band FMCW radar with micrometer accuracy”, *European Radar Conference (EuRAD)* 2015, pp. 277–280.
58. J. Grzyb, K. Statnikov, N. Sarmah, B. Heinemann and U. R. Pfeiffer, “A 210–270 GHz circularly polarized FMCW radar with a single-lens-coupled SiGe HBT chip”, *IEEE Trans. Terahertz Sci. Technol.* 6, pp. 771–783 (2016)
59. H. Aggrawal, P. Chen, M. M. Assefzadeh, B. Jamali and A. Babakhani, “Gone in a Picosecond: Techniques for the Generation and Detection of Picosecond Pulses and Their Applications”, in *IEEE Microwave Magazine*, vol. 17, no. 12, pp. 24–38, (2016), <https://doi.org/10.1109/MMM.2016.2608764>